



## **Ru(II)-Fe(III) Bimetallic Complex as a Multifunctional Device for Detecting, Signal Amplifying, and Degrading Oxalate**

Journal:	<i>Analyst</i>
Manuscript ID:	AN-ART-02-2014-000350.R1
Article Type:	Paper
Date Submitted by the Author:	03-Jun-2014
Complete List of Authors:	Chow, Cheuk-Fai; The Hong Kong Institute of Education, Department of Science and Environmental Studies Ho, Pui-Yu; The Hong Kong Institute of Education, Department of Science and Environmental Studies Gong, Chengbin; Southwest university, The college of chemistry & Chemical engineering

Cite this: DOI: 10.1039/c0xx00000x

www.rsc.org/xxxxxx

ARTICLE TYPE

# Ru(II)-Fe(III) Bimetallic Complex as a Multifunctional Device for Detecting, Signal Amplifying, and Degrading Oxalate

Cheuk-Fai Chow<sup>\*a,b</sup>, Pui-Yu Ho<sup>a,b</sup>, Cheng-Bin Gong<sup>c</sup>

Received (in XXX, XXX) Xth XXXXXXXXX 20XX, Accepted Xth XXXXXXXXX 20XX

DOI: 10.1039/b000000x

A tetranuclear bimetallic complex,  $[\text{Ru}^{\text{II}}(\text{Bubpy})(\text{CN})_4]_2-[\text{Fe}^{\text{III}}(\text{H}_2\text{O})_3\text{Cl}]_2 \cdot 4\text{H}_2\text{O}$  (**1**) has been synthesized and characterized. It was found to be a multifunctional device that can detect, signal amplify, and degrade an organic pollutant, oxalate. Results of the chemosensing studies of **1** toward common anions show that only oxalate selectively induces a naked-eye colorimetric and luminometric responses with method detection limits down to 78.7 and 5.5 ppm, respectively from **1**. Meanwhile, results of the photo-degradation studies of **1** toward oxalate show that the dissolved organic carbon content of oxalate decreased and reached completely mineralization into  $\text{CO}_2$  within 6 hours. Complex **1** was also found as the catalyst to amplify the detection signal toward oxalate. Through the photoassisted Fenton reaction by **1**, methyl orange, an additional coloring agent, could be degraded so that the visual detection limit of **1** toward oxalate was magnified 50 times from 100 to 2 ppm. All the detection, degradation, mineralization and signal amplification were found applicable in real water bodies such as river, pond and underground water with excellent recoveries and relative standard deviation.

## Introduction

The efficient detection and degradation of persistent industrial pollutants are major challenges faced by the world today.<sup>1-4</sup> Stable chemosensors with high sensitivity and selectivity as well as advanced catalysts that can quickly oxidize and mineralize organic contaminants are in high demand. In this context, a multifunctional device that (i) can selectively monitor the level of pollutants, (ii) can magnify weak detection signal, and (iii) can subsequently degrade pollutants into harmless substances is highly desirable.<sup>5-7</sup> This allosteric approach can trim down the loading of chemicals (e.g., chemosensors,  $\text{H}_2\text{O}_2$ ), catalysts (e.g., transition metal complexes), and energy usage (e.g., continuous UV irradiation) through traditional sensing and degradation.

Research attention has been focused on the development of chemosensors for the in situ monitoring of pollutants.<sup>8-9</sup> Indicator displacement assay (IDA),<sup>10-21</sup> is a relatively new chemosensing approach that has been applied to determine anions,<sup>10,13,16-18,20</sup> neutral organic molecules,<sup>21</sup> zwitterions,<sup>14,19</sup> and other molecules<sup>11,12,15</sup>. IDA involves the initial binding of an indicator to a receptor, forming an "ensemble." A competitive analyte (the targeted contaminant) is then introduced into the system, thus causing the displacement of the indicator from the receptor, which in turn supplies an optical signal. IDA approaches feature good analyte selectivity and high sensitivity. They also provide rapid and reliable assays. Research groups led by Anslyn,<sup>10-12</sup> Fabbri, <sup>13-15</sup> and Martinez-Manez<sup>16-18</sup> are the pioneers of this chemosensing assay.

The elimination of harmful chemicals should immediately proceed following their discovery to deal with industrial waste problems. Fenton reaction is an innovative method for chemical waste treatment that is extremely useful in cases involving substances that are resistant to conventional degradation technologies.<sup>22-24</sup> Fenton reactions by transition metal complexes<sup>23-24</sup> refer to those oxidative reactions that generate highly oxidizing species, such as hydroxyl ( $\cdot\text{OH}$ ), superoxide

( $\cdot\text{O}_2^-$ ) and/or hydroperoxyl ( $\text{HO}_2\cdot$ ) radicals under UV and/or Vis irradiation in the presence of a metal catalyst, for the destruction and ultimate mineralization of targeted contaminants. Although the reaction has been widely utilized to combat a variety of pollutants in water, wastewater, and soil,<sup>22</sup> this degradation method usually suffers from overdosage of chemicals (e.g.,  $\text{H}_2\text{O}_2$ ), catalyst losses (e.g., transition metal complexes), and energy usage (e.g., continuous UV irradiation). Recently, Liu et al. reported a Fenton-like degradation system using cyano-complex,  $\text{KFe}^{\text{III}}\text{Fe}^{\text{II}}(\text{CN})_6$ , as an active catalyst for degrading rhodamine B, an organic color reagent.<sup>23-24</sup>

Catalytic signal amplification is an evolving analytical method for reporting trace amounts of analyte with high selectivity and sensitivity.<sup>25-32</sup> It is the interaction of an analyte with a chemosensor that initiates a process resulting in the formation of a large number of reporter molecules through catalysis. This scenario is an emerging technique that has been used to detect and quantify various analytes in aqueous solution. Enzyme-linked immunosorbent assay (ELISA) is one of the most common signal amplification routines.<sup>33</sup> In contrast to this aforementioned biochemical method, supramolecular chemical catalysis that involves robust signal amplification is highly attractive. Some chemical systems that can amplify originally weak input signals have been reported by Anslyn,<sup>25-26</sup> Prins,<sup>27-28</sup> and others<sup>29-32</sup>. However, a smart molecular device that can amplify the reporting signal and simultaneously degrade pollutants through simple chemical design is highly desirable.

Oxalic acid is an organic acid that is widely used in many industrial processes, such as in printing and dyeing, production of pharmaceuticals, extraction of rare earth metals from their ores, and synthesis of fine chemicals.<sup>34-35</sup> With the expansion of biomedical industries and metallurgy, demand for oxalic acid has increased in recent decades. In 2009, the global demand for oxalic acid was approximately 450,000 tons, whereas the demand in Mainland China exceeded 300,000 tons.<sup>36</sup> The safe disposal of spent oxalic acid is a challenging industrial, environmental, and public health problem. The consumption of seafood and water

with high levels of oxalic acid can cause food poisoning. In mammals, oxalic acid has an oral LD<sub>50</sub> of 600 mg/kg body weight.<sup>37</sup> The excessive accumulation of oxalic acid in the human body can cause a variety of health disorders, such as renal failure, urinary stone disease, and pancreatic insufficiency.<sup>38–40</sup> The deposition of calcium oxalate can induce nephrocalcinosis.<sup>39</sup>

In this work, we synthesize a bimetallic complex, Ru<sup>II</sup>-Fe<sup>III</sup> complex, and develop a sensing/catalytic degradation approach called indicator/catalyst displacement assay (ICDA) for the design of multifunctional molecular devices that feature chemosensing, signal amplifying, and advanced oxidation catalytic properties for dealing with the aforementioned pollutants. The concept of the ICDA resembles antibody-based immunoassays<sup>33</sup> and allosteric catalytic reactions.<sup>29–31</sup> In the ICDA, a Fe(III) receptor that is also a catalyst was first allowed to bind reversibly to a Ru(II)-indicator that is also an inhibitor. Then, a competitive analyte, oxalic acid, is introduced into the system, causing the displacement of the Fe(III) receptor (catalyst) from the indicator (inhibitor), which in turn activates the indicator, as well as the catalyst. Ultimately, the level of the analyte can be monitored, the signal can be amplified, and the pollutant can be degraded into harmless components in a one-step process. Results showed that the bimetallic complex was able to produce naked-eye colorimetric responses specifically to oxalic acid down to 78.7 ppm in aqueous system and could subsequently degraded and mineralized the pollutant into CO<sub>2</sub> by only using atmospheric O<sub>2</sub> as oxidant under UV irradiation within 6 h (5% dissolved organic carbon, so called DOC<sub>95</sub>). Through the catalytic signal amplification, the detection limit of **1** toward oxalate was magnified 50 times from 100 ppm to 2 ppm. The ICDA concept was found workable in real water bodies such as river, lake, and underground water.

## Experimental Section<sup>41</sup>

**[Ru<sup>II</sup>(<sup>t</sup>Bubpy)(CN)<sub>4</sub>]<sub>2</sub>-[Fe<sup>III</sup>(H<sub>2</sub>O)<sub>3</sub>Cl]<sub>2</sub>·4H<sub>2</sub>O (**1**).** A mixture of K<sub>2</sub>[Ru<sup>II</sup>(<sup>t</sup>Bubpy)(CN)<sub>4</sub>] (0.276 g, 0.5 mmol) and anhydrous FeCl<sub>3</sub> (0.081 g, 0.5 mmol) was stirred in deionized water (50 mL) room temperature for 60 min. Blue precipitates obtained by filtration were washed with deionized water, acetone and diethyl ether and were air-dried. Yield: 0.261 g (76 %). IR (KBr): ν<sub>C≡N</sub> = 2030, 2076, and 2114 cm<sup>-1</sup>. ESI-MS (+ve mode): m/z 620.0 {2H<sup>+</sup>•[Ru(<sup>t</sup>Bubpy)(CN)<sub>4</sub>]<sub>2</sub>-[Fe(H<sub>2</sub>O)<sub>3</sub>Cl]<sub>2</sub>} (mass = 1240.1 gmol<sup>-1</sup>; charge = +2). Anal. Calcd. for C<sub>44</sub>Cl<sub>2</sub>Fe<sub>2</sub>H<sub>60</sub>N<sub>12</sub>O<sub>6</sub>Ru<sub>2</sub>·8H<sub>2</sub>O (**1**): C, 38.24; H, 5.54; N, 12.16. Found: C, 37.98; H, 5.55; N, 12.00.

**UV-vis Spectroscopic and Spectrofluorimetric Titrations.** All solvents used in UV-vis spectroscopic and spectrofluorimetric titrations were KCl/HCl pH 1.5 (0.5M) buffer. Measurements were taken after equilibrium had been reached between the receptor and substrate. A 1:1 receptor-substrate interaction was analyzed according to Benesi-Hildebrand equations<sup>41</sup> for UV-vis spectroscopic titration or spectrofluorimetric titration.

**Chemosensing Selectivity of Complex **1** towards Various Analytes.** A series of analytes (oxalate, glyoxylic acid, pyruvic acid, potassium tartrate, potassium acetate, NCS<sup>-</sup>, H<sub>2</sub>PO<sub>4</sub><sup>-</sup>, Br<sup>-</sup>, NO<sub>3</sub><sup>-</sup>, N<sub>3</sub><sup>-</sup> and SO<sub>4</sub><sup>2-</sup>) (0 to 9.52 × 10<sup>-3</sup> M) were mixed with complex **1** solutions (2.17 × 10<sup>-4</sup> M). The titrations were carried out in a 2:1 ratio of ethanol/pH 1.5 aqueous buffer mixture at room temperature. Spectrofluorimetric changes of the resulting mixtures were plotted as a function of mole fraction of the

analyte. The luminescent responses of complex **1** to the analytes were also obtained by digital photography.

**Photocatalytic Degradation of Analytes by Complex **1**.** All experiments were conducted in a 125 mL conical flask with irradiation source, 200 W Hg(Xe) ultraviolet-visible lamp (Newport). The whole setup was shielded from surrounding light. The distance between the lamp and the test solution was about 10 cm. Generally, a 100 mL test solution was stirred during the photocatalytic experiments, in which the concentration of complex **1** was equal to 1.79 × 10<sup>-4</sup> M, while oxalate, glyoxylic acid, pyruvate, L-tartrate and acetate were 1.79 × 10<sup>-3</sup> M. The pH value of the test solution was adjusted at 1.5. Dissolved organic carbon (DOC) of the system was obtained at regular intervals to understand catalytic efficiency. All samples were analyzed immediately to avoid errors due to further reactions.

### Catalytic signal amplification of Complex **1** toward Oxalate.

A series of oxalate [0 to 2.17 × 10<sup>-3</sup> M (0 to 400ppm)] were mixed with complex **1** (2.17 × 10<sup>-4</sup> M) and methyl orange (2.17 × 10<sup>-5</sup> M) mixture. The studies were carried out in pH 1.5 aqueous buffer at room temperature. Each solution was irradiated under 200 W Hg(Xe) ultraviolet-visible lamp (Newport) for 180 min. The whole setup was shielded from surrounding light. The distance between the lamp and the test solution was about 30 cm. UV-vis absorption spectra and their intensity at 510 nm were recorded at fixed time intervals.

## Results and Discussion

**Synthesis of Tetranuclear Bimetallic Complex **1**.** By demonstrating a convenient way by using the ICDA approach in integrating a chemodosimeter and photo-oxidative catalyst, herein we report a novel tetranuclear bimetallic complex, [Ru<sup>II</sup>(<sup>t</sup>Bubpy)(CN)<sub>4</sub>]<sub>2</sub>-[Fe<sup>III</sup>(H<sub>2</sub>O)<sub>3</sub>Cl]<sub>2</sub>·4H<sub>2</sub>O (**1**). Two [Ru<sup>II</sup>(<sup>t</sup>Bubpy)(CN)<sub>4</sub>]<sub>2</sub><sup>2-</sup> luminescent centers cyano-bridging with two FeCl<sub>3</sub> recognition centers gave selectivity binding toward oxalate in aqueous medium. Through the control of the thermodynamics between Ru<sup>II</sup> and Fe<sup>III</sup> complex, chemodosimetric and photocatalytic properties of complex **1** toward oxalate could be manipulated.

The tetranuclear complex **1** was formed by stirring 1 equivalent of FeCl<sub>3</sub> with 1 equivalent of K<sub>2</sub>[Ru(<sup>t</sup>Bubpy)(CN)<sub>4</sub>] in deionized water in an open atmosphere at room temperature (SI. Scheme 1). The complex was isolated as an air-stable blue solid in good yield (76 %). It is soluble in DMSO, DMF, MeOH and EtOH but is virtually insoluble in acetone, acetonitrile, chloroform, dichloromethane and water. The integrity of its tetranuclear form in such a medium is demonstrated by the electrospray-MS showing peaks at 620.0 m/z representing {2H<sup>+</sup>•[Ru(<sup>t</sup>Bubpy)(CN)<sub>4</sub>]<sub>2</sub>-[Fe(H<sub>2</sub>O)<sub>3</sub>Cl]<sub>2</sub>}<sup>2+</sup> (mass = 1240.1 gmol<sup>-1</sup>; charge = +2) (SI. Figure 1). Furthermore, spectrofluorimetric titrations (Job's plot) of K<sub>2</sub>[Ru(<sup>t</sup>Bubpy)(CN)<sub>4</sub>] with FeCl<sub>3</sub> solution show that the solvated form of the complex is in a ratio of 1:1 [Ru(II):Fe(II)] (SI. Figure 2). Formation of the cyano-bridged bimetallic complex is also confirmed by IR spectroscopic analysis where the ν<sub>C≡N</sub> of K<sub>2</sub>[Ru(<sup>t</sup>Bubpy)(CN)<sub>4</sub>] at 2042, 2058, and 2093 cm<sup>-1</sup> were shifted to 2030, 2076, and 2114 cm<sup>-1</sup> in complex **1**. The tetranuclear bimetallic complex was successfully characterised by positive-ion ESI-mass spectrometry, IR and gave satisfactory elemental analyses

**Electronic Absorption and Luminescent Properties of 1.** The absorption spectra of complex **1** and its precursors are shown in SI. Figure 3a. From 200 to 465 nm, the UV-vis spectrum of **1** is a superposition of the spectra of  $K_2[Ru^{\text{II}}(\text{Bubpy})(\text{CN})_4]$  and  $\text{FeCl}_3$ . But the dominating feature of **1** is the broad metal-metal charge transfer (MMCT) band in the visible range.<sup>42–43</sup> The occurrence of this band puts it into class II of the mixed-valent species.<sup>41–42</sup> The direction of the MMCT is suggested as  $\text{Ru}(\text{II}) \rightarrow \text{Fe}(\text{III})$ . A low-energy emission band at ca. 550–750 nm dominates the emission spectrum of complex **1**. With reference to previous spectroscopic works, the low-energy emission band is assigned as a  $[\pi^*(\text{diimine}) \rightarrow d\pi(\text{Ru})]$  <sup>3</sup>MLCT emission.<sup>44</sup> SI. Figure 3b shows the <sup>3</sup>MLCT emission spectra of complex **1** and its precursors. The decrease in <sup>3</sup>MLCT emission intensity of **1** is the consequence of coordination of the diamagnetic  $\text{Fe}(\text{III})$  quencher to the  $\text{Ru}(\text{II})$ -diimine chromophore.<sup>45</sup>

### Chemodosimetric Properties of Complex 1 toward Oxalate.

Figures 1a–b show the colorimetric and luminescent responses of **1** to oxalate ( $\text{HC}_2\text{O}_4^-$ ). With the addition of oxalate to **1** to an aqueous ethanol solution at pH 1.5, the intensity of its metal-metal charge transfer (MMCT) band declines and results in a blue to pale yellow colorimetric response (Figure 1a). Meanwhile, the addition also perturbs the <sup>3</sup>MLCT transition of **1** with a significant enhancement in intensity resulting in an intense orange colored emission (Figure 1b). The fitting of the UV-vis spectroscopic responses to a 1:2 Benesi–Hildebrand equation<sup>41</sup> yields the overall formation constant,  $\log K_{\text{overall}}$ , as  $3.43 \pm 0.03 \text{ M}^{-1}$  between **1** and oxalate (Figure 1c). This result suggests that each  $\text{Fe}(\text{III})$  center in the tetranuclear complex binds one molecule of oxalate. Through the UV-vis spectroscopic and spectrofluorometric methods, the method detection limits (MDL) of **1** toward oxalate were found as 78.7 and 5.5 ppm via Hubaux and Vos method.<sup>41</sup> The visible detection limit, which was judged by naked eye, of **1** toward oxalate was  $\sim 100$  ppm (Figure 4c).

Figures 1d and e summarizes the spectrofluorometric titrations of **1** with oxalate and common analytes (glyoxylic acid, pyruvic acid, potassium tartrate, potassium acetate,  $\text{K}_2\text{SO}_4$ ,  $\text{KH}_2\text{PO}_4$ ,  $\text{KNO}_3$ , KCN, KSCN,  $\text{KN}_3$  and KBr) in the aqueous

**Table 1.** Binding constants ( $\log K_{\text{overall}}$ ) and Gibbs free energy changes ( $\Delta G^\circ$ ) for the complexation of various analytes and  $K_2\text{Ru}(\text{Bubpy})(\text{CN})_4$  by  $\text{FeCl}_3$ .

Acceptor	Donor	$\log K_{\text{overall}}^b$	$\Delta G^\circ / \text{kJmol}^{-1}$	
1	$\text{FeCl}_3$	Oxalate	3.52	-20.1
2	$\text{FeCl}_3$	$K_2\text{Ru}(\text{Bubpy})(\text{CN})_4$	3.15	-18.0
3	$\text{FeCl}_3$	Pyruvic acid	2.55 <sup>b</sup>	-14.5
4	$\text{FeCl}_3$	$\text{KH}_2\text{PO}_4$	2.33	-13.3
5	$\text{FeCl}_3$	KCN	1.91	-10.9
6	$\text{FeCl}_3$	$\text{KN}_3$	1.47 <sup>c</sup>	-8.16
7	$\text{FeCl}_3$	Potassium tartrate	1.36	-7.7
8	$\text{FeCl}_3$	Potassium acetate	0.96	-5.5
9	$\text{FeCl}_3$	KSCN	0.75	-4.3
10	$\text{FeCl}_3$	Glyoxylic acid	0.54	-3.1
11	$\text{FeCl}_3$	$\text{K}_2\text{SO}_4$	0.24	-1.4
12	$\text{FeCl}_3$	$\text{KNO}_3$	---	---
13	$\text{FeCl}_3$	KBr	---	---

<sup>a</sup>Binding strengths were measured by UV spectroscopic titration and calculated with Benesi–Hildebrand 1:1 equation. <sup>b</sup>Binding strengths were measured by spectrofluorimetric titration and calculated with Benesi–Hildebrand 1:1 equations. <sup>c</sup>Binding strengths were measured by UV spectroscopic titration and calculated with Benesi–Hildebrand 1:2 equations. <sup>d</sup>All the titrations were conducted in aqueous KCl/HCl buffer at pH 1.5 at 298 K. <sup>e</sup>Too small to be determined.

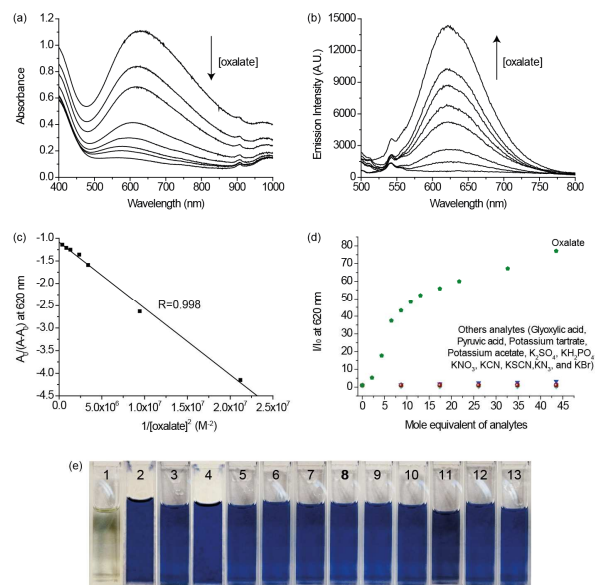


**Figure 1.** (a) UV-vis spectroscopic and (b) spectrofluorimetric titrations of **1** ( $1.08 \times 10^{-4} \text{ M}$ ) with oxalate (0 to  $3.24 \times 10^{-2} \text{ M}$ ). (c) The best fitted  $A_0/(A-A_0)$  versus  $1/[\text{oxalate}]^2$  plot with  $\log K = 3.43 \pm 0.03$  at 620 nm (the slope and y-intercept are -1.084 and  $-1.47 \times 10^{-7} \text{ M}^2$ , respectively). (d) Summary of spectrofluorometric titration ( $I/I_0$  at 620 nm) of **1** ( $2.17 \times 10^{-4} \text{ M}$ ) to various analytes monitored as a function of the increase in their concentration. (e) Photos of the colorimetric responses of complex **1** ( $2.17 \times 10^{-4} \text{ M}$ ): (1) **1** + oxalate, (2) **1** only; (3–13) **1** + glyoxylic acid, pyruvic acid, potassium tartrate, potassium acetate,  $\text{K}_2\text{SO}_4$ ,  $\text{KH}_2\text{PO}_4$ ,  $\text{KNO}_3$ , KCN, KSCN,  $\text{KN}_3$ , and KBr. All luminometric and colorimetric responses were recorded in aqueous ethanol (1:2 v/v) (1.00 mL of aqueous KCl/HCl buffer at pH 1.5 + 2.00 mL of ethanol) at 298 K. Excitation at 468 nm.

ethanol solution. Among these analytes, only oxalate produces a spectrofluorometric response through its reaction with **1**; the other analytes are unable to induce any spectrofluorometric changes in **1** (Figure 1d). Moreover, the responses of **1** toward a mixture of oxalate and analytes showed similar results as that toward oxalate alone (SI. Figure 4, sets 1 & 2). These results reveal that the selectivity of **1** toward oxalate and the common analytes does not interfere with the signaling responses of **1** toward the detection of oxalate. Most importantly, the detection of oxalate by **1** can be observed by the naked eye via colorimetric changes in the solution (Figure 1e).

Figure 2 shows the proposed recognition and signaling mechanism of complex **1** toward oxalate. The close resemblance of the UV-vis and luminescent responses of the “**1**-oxalate-mixture” to those of  $K_2\text{Ru}(\text{Bubpy})(\text{CN})_4$  and the subsequent observation of  $[\text{Ru}^{\text{II}}(\text{Bubpy})(\text{CN})_4]^{2+}$  in the electrospray-MS of the mixture (SI. Figure 5;  $m/z$  512.9  $[\text{M} + \text{K}]^+$ ) suggest that all the cyanide bridges between  $\text{Ru}(\text{II})$  and  $\text{Fe}(\text{III})$  in the tetranuclear complex are cleaved after oxalate molecules bind to the  $\text{Fe}(\text{III})$  centers. The substrate selectivity of the binding-induced dissociation is most probably attributable to the relative stability of the  $\text{Ru}(\text{II})$ - $\text{Fe}(\text{III})$  complex compared with that of the  $\text{Fe}^{\text{III}}$ -analyte adducts. As only  $\text{Fe}^{\text{III}}$ -oxalate exhibits a  $\Delta G^\circ$  smaller than that of **1**, the driving force for the cleavage of **1** by oxalate is the formation of highly stable  $\text{Fe}(\text{III})$ -oxalate species. (Table 1, SI. Figures 6–16)

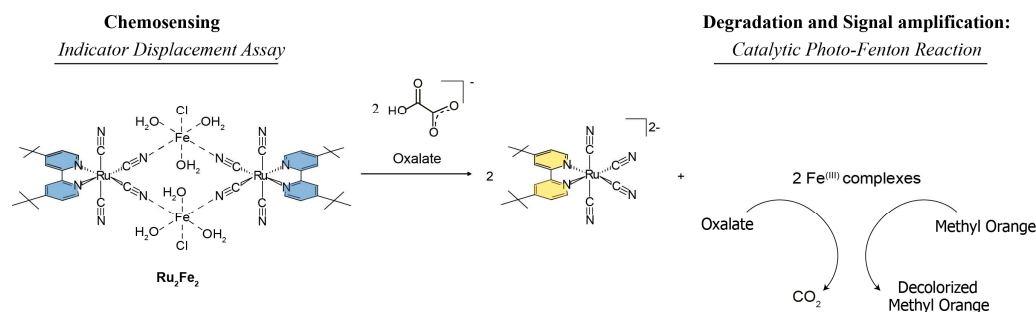


**Figure 2.** Proposed ICDA of **1** toward oxalate. The mechanism is composed of chemosensing, degradation, and signal amplification.

### Photocatalytic degradation of Oxalate by Complex **1**.

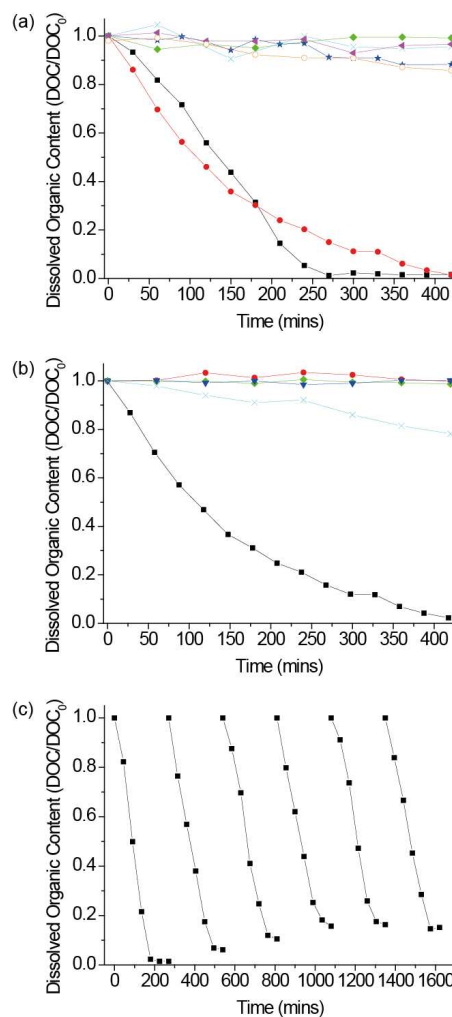
Photo-degradation studies were conducted by investigating the effect of initial oxalate concentration ( $4.16 \times 10^{-4}$  M) using different catalysts at pH 1.5 buffer (KCl, HCl 0.5 M) in various working conditions. In the presence of **1** under UV-vis irradiation at room temperature, the DOC content of the solution mixture decreased rapidly in the first 250 min and gradually dropped afterwards. The time required for the 95% mineralization ( $\text{DOC}_{95}$ ) of oxalate was approximately 360 min [Figure 3a curve (●)]. A similar experiment was conducted in the presence of  $\text{FeCl}_3$  and oxalate under UV irradiation; the DOC content of the solution mixture decreased in a similar pattern as **1** [Figure 3a curve (■)].

However, when an exact experiment was conducted in the presence of  $\text{K}_2\text{Ru}(\text{Bubpy})(\text{CN})_4$ , the DOC content of the solution mixture remained unchanged after 7 h of treatment [Figure 3 curve (◆)]. Based on these results, we suggest that the remediation of oxalate by **1** is due to the release of  $\text{Fe}(\text{III})$  complexes. Furthermore, the conditions of (i) dark, (ii) dark with heat ( $50^\circ\text{C}$ ), and (iii) nitrogen atmosphere, all show no evidence of any degradation [Figure 3a curves (×), (◄) and (★) respectively]. Hence, the degradation of oxalate is most probably due to the superoxide ion radical,  $\text{O}_2^-$ , and/or to the hydroxyl radical via photoassisted Fenton mechanism with the help of UV-vis irradiation [(i)  $\text{Fe}^{2+} + \text{O}_2 \rightarrow \text{Fe}^{3+} + \text{O}_2^-$ ; (ii)  $2\text{O}_2^- + 2\text{H}^+ \rightarrow \text{H}_2\text{O}_2 + \text{O}_2$ ; (iii)  $\text{Fe}^{2+} + \text{H}_2\text{O}_2 \rightarrow \text{Fe}^{3+} + \text{OH}^- + \text{HO}\cdot$ ].<sup>46–48</sup>

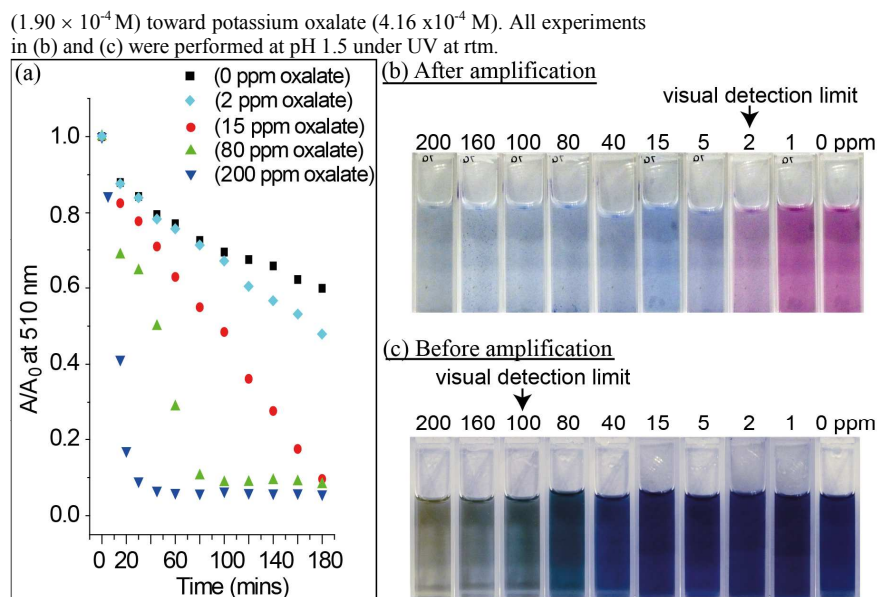
Organic carboxylic acids/carboxylates were used as organic interferences to understand the selectivity of the photodegradation of **1** toward oxalate. Figure 3b summarizes the change in the DOC content of oxalate, glyoxylic acid, pyruvic acid, potassium tartrate, and potassium acetate against the time of exposure to **1** under UV-vis irradiation at room temperature and open atmosphere. Among all the analytes, only oxalate was selectively degraded with a significant decrease in its DOC content through its reaction with **1**, whereas the other substances were unable to induce any changes in significant organic content in the presence of **1**. The selective degradation is believed to be related to the chemosensing properties of **1** toward oxalate (Figure 2). Introducing oxalate into the system caused the activation of the  $\text{Fe}(\text{III})$  catalyst by breaking the cyano-linkages from  $[\text{Ru}(\text{Bubpy})(\text{CN})_4]^{2-}$ . Subsequently, oxalate was degraded into  $\text{CO}_2$  in this allosteric process. Although other analytes were introduced into the system, **1** remained intact, and the cyano-bridged  $\text{Fe}(\text{III})$  catalyst remained inactive. The above experiments verify that **1** is a selective photodegradation catalyst for oxalate.

Figure 3c shows the repeatability of the action of **1** toward oxalate. The experiments were performed with the catalyst continuously recycled six times. Afterwards, the efficiency still

reached 85.0% although the degradation of oxalate decreased, thus indicating that the catalyst exhibited repeatable efficiency.



**Figure 3.** (a) DOC during the degradation of oxalate under various conditions. (●) In the presence of **1** ( $1.90 \times 10^{-4}$  M), (■)  $\text{FeCl}_3$  ( $1.90 \times 10^{-4}$  M) and (◆)  $\text{K}_2\text{Ru}(\text{Bubpy})(\text{CN})_4$  ( $1.90 \times 10^{-4}$  M) under UV irradiation at room temperature. In the presence of **1** ( $1.90 \times 10^{-4}$  M) under (×) dark condition at room temperature, (◄) dark condition at  $50^\circ\text{C}$ , and (★) under UV irradiation at room temp with saturation of  $\text{N}_2$  (○). Control experiment was conducted at pH 1.5 with oxalate ( $4.16 \times 10^{-4}$  M) under UV at room temperature and open atmosphere. (b) Selective degradation properties of **1** ( $1.90 \times 10^{-4}$  M) toward different organic carboxylate ( $4.16 \times 10^{-4}$  M), (■) potassium oxalate, (●) potassium acetate, (▼) potassium tartrate, (◆) pyruvic acid, and (×) glyoxylic acid. (c) Repeatability of **1**



**Figure 4.** (a) Spectroscopic changes with time of **1** solution added with methyl orange (1:1 mol/mol) in the presence of oxalate (0 ppm to 200 ppm). All titrations were conducted in aqueous buffer (pH 1.5) under UV-vis at room temperature. (b) Photos of the colorimetric responses observed in Figure 4(a). (c) Photos of colorimetric response observed in Figure 1(b). The visual detection limit of oxalate was amplified  $\sim 50$  times when methyl orange was used as a signaling amplification agent.

**1** solution added with methyl orange against time under UV-vis irradiation. In the presence of oxalate ( $\geq 2$  ppm),  $\lambda_{\text{abs}}$  at 510 nm of the solution decreased with time. However,  $\lambda_{\text{abs}}$  remains unchanged with respect to time in the absence or presence of small amounts of oxalate ( $\leq 1$  ppm). The complete decolorization (95% of  $\lambda_{\text{abs}}$  at 510 nm) of the solution was achieved in 180 min when 15 ppm oxalate was present in the mixture. A fast decolorization rate of the solution was achieved in 100 min when 80 ppm oxalate was present in the mixture (Figure 4a). Figure 4b shows the naked-eye responses of the **1** solution added with methyl orange toward various oxalate concentrations after 180 min UV-vis irradiation. The visual detection limit of the solution toward oxalate is 2 ppm. Figure 4c shows the colorimetric responses, before the amplification, of the **1** solution toward various oxalate concentrations (their UV-vis spectroscopic spectra were showed in Figure 1a). The visual detection limit of **1**, before the amplification, toward oxalate is 100 ppm. As revealed by these results, sensitivity can be amplified around 50 times, that is, from 100 ppm to 2 ppm through this catalytic amplification process.

**Detection, amplification, and photo-degradation of oxalate in real water samples by 1.** For final verification of the ICDA idea, **1** was used to examine the detection, signal amplification, and photo-degradation of oxalate in lake, river, and underground water samples. All the water samples were collected in Hong Kong, China. The samples were filtered through  $0.45 \mu\text{m}$  pore-size membrane filters (Pall Corporation) to remove insoluble substances before the examination.

As for the studies of the spectrofluorometric detection of oxalate in the real samples by **1**, all the samples spiked with 33.3 ppm oxalate were analyzed by **1** in a 2:1 ratio of ethanol/pH 1.5 aqueous buffer mixture at room temperature with a developed calibration curve (SI. Figure 17). The analytical results show that **1** is able to measure the concentrations of spiked oxalate in all the real water samples with a good recovery and relative standard

Figure 3c shows the repeatability of the action of **1** toward oxalate. The experiments were performed with the catalyst continuously recycled six times. Afterwards, the efficiency still reached 85.0% although the degradation of oxalate decreased, thus indicating that the catalyst exhibited repeatable efficiency.

**Catalytic signal amplification of Complex 1 towards Oxalate.** With the help of methyl orange as an additional coloring agent, complex **1** was applied to amplify the signal toward the detection of oxalate. We expected that the organic chromophores of methyl orange can be destroyed by reacting with hydroxyl radicals through the aforementioned catalytic photoassisted Fenton reaction<sup>49–50</sup>; hence, the organic chromophores of methyl orange loses its color ( $\lambda_{\text{abs}}$  at 510 nm), thus resulting in a sharp magnified color change (Figure 2). Figure 4a shows the UV-vis spectroscopic changes in the

deviation (RSD, %) as 92.4 – 115.8 % and 2.24 – 2.76 %, respectively (Table 2). These results indicate the suitability and practicality of **1** for the detection of oxalate from real water samples without any interference from other environmentally relevant competitive anions.

For the studies of the photo-degradation of oxalate in the real water samples by **1**, all the samples spiked with 767 ppm oxalate were analyzed in pH 1.5 medium at room temperature. In the

**Table 2.** Results of oxalate detecting/degrading/signal amplifying lake, river, and underground water samples with **1**.

Detection				
Water samples	Oxalate added ( $\mu\text{g/L}$ )	Oxalate found (ppm)	Recovery (%)	RSD (%)
lake	33.3	$31.5 \pm 0.9$	94.6	2.76
river	33.3	$38.6 \pm 1.0$	115.8	2.60
underground	33.3	$30.8 \pm 0.7$	92.4	2.24
Degradation				
Water samples	Oxalate added ( $\mu\text{g/L}$ )	Oxalate left (ppm)	DOC <sub>95</sub> (min)	
lake	767.0	0.0	175	
river	767.0	0.0	205	
underground	767.0	0.0	200	
Amplification				
Water samples	Oxalate added ( $\mu\text{g/L}$ )	Oxalate found (ppm)	Recovery (%)	RSD (%)
lake	10.0	$10.1 \pm 0.07$	101.4	6.42

river	3.3	3.5 ± 0.09	103.9	9.18
underground	13.3	12.7 ± 0.07	95.1	6.89

presence of **1** under 200 W UV-vis irradiation, the DOC content of the samples (river, lake, and underwater) decreased rapidly in the first 2 h. The times required for the 95% mineralization (DOC<sub>95</sub>) of oxalate were approximately 175, 205, and 200 min for the lake, river, and underground water samples respectively (SI. Figure 18). The negative values of DOC obtained after the reaction can be explained as the result of destructing the existing organic matters in the real samples. These results indicate the degradation of oxalate by **1** does not interfere by the presence of organic matters in the real water samples.

The signal amplification of oxalate in the real water samples by **1** was performed by spiking small amount of oxalate in the river (3.3 ppm), lake (10.0 ppm), and underground (13.3 ppm) water samples in the presence of methyl orange at a 2:1 ratio of ethanol/pH 1.5 aqueous buffer mixture under 200 W UV-vis irradiation with a developed calibration curve (SI. Figure 19). The results show that **1** is able to amplify tiny amount of oxalate in all the real water samples with an excellent recovery and good relative standard deviation (RSD, %) as 95.1 – 103.9 % and 6.42 – 9.18 %, respectively (Table 2).

For further validation of the application of complex **1** in real water samples, *in vivo* toxicity assay of the complex towards Japanese Medaka (*Oryzias latipes*) was conducted. Seven medaka larvae (ca. 4 – 5 mm in length) were held in each of six-well cell culture plate with a suspension of the complex **1** of 0 (as a control), 1, 10 and 100 mg/mL for 7 days. No abnormal behavior, nor mortality, of the fish was ever observed within the 7-days exposure period (SI. Figure 20). Complex **1** does not cause any apparent adverse effect to the organism.

## Conclusions

A tetranuclear heterobimetallic Ru(II)-Fe(III) donor-acceptor complex was synthesized, characterized and applied in the study reported herein. Complex **1** appears to be the first multifunctional device that can simultaneously detect, signal amplify, and degrade oxalate in real water sample. The indicator/catalyst displacement assay (ICDA), in which one metal center acting as a receptor that is also an inhibitor is bridged to another metal center responsible for signal transduction that is also a catalyst, seems to be a versatile way of designing such type of multifunctional devices. To the best of our knowledge, no example of such multifunctional molecular device has been reported in previous studies. Efforts are being made on studying the feasibility of designing other cyano-bridged bimetallic complexes with similar multifunctional properties for other pollutants (e.g., cyanide, azo-dyes, amines, carboxylic acids, and organophosphate pesticides).

## Acknowledgement

The work described in this paper was funded by a grant from the Hong Kong Institute of Education (Project Nos. 04020 and R3444), and a grant from the Research Grants Council of Hong Kong SAR, China (ECS no. 800312). Special thanks also go to Dr. Doris W. T. Au (City University of Hong Kong) for the supply of Medaka embryos

## Notes and references

<sup>a</sup>Department of Science and Environmental Studies, The Hong Kong Institute of Education, 10 Lo Ping Road, Tai Po Hong Kong SAR, China Fax: (+852) 29487676; Tel: (+852) 29487671; E-mail: cfchow@ied.edu.hk

<sup>b</sup>Centre for Education in Environmental Sustainability, The Hong Kong Institute of Education, 10 Lo Ping Road, Tai Po Hong Kong SAR, China.

<sup>c</sup>College of Chemistry and Chemical Engineering, Southwest University, Chong Qing, China.

† Supporting information including the synthetic procedures, electrospray mass spectra, spectroscopic/spectrofluorimetric analyses, all of the UV-vis spectroscopic and spectrofluorometric titrations and toxicity tests are available free of charge in the supporting sections are available. See DOI: 10.1039/b000000x/

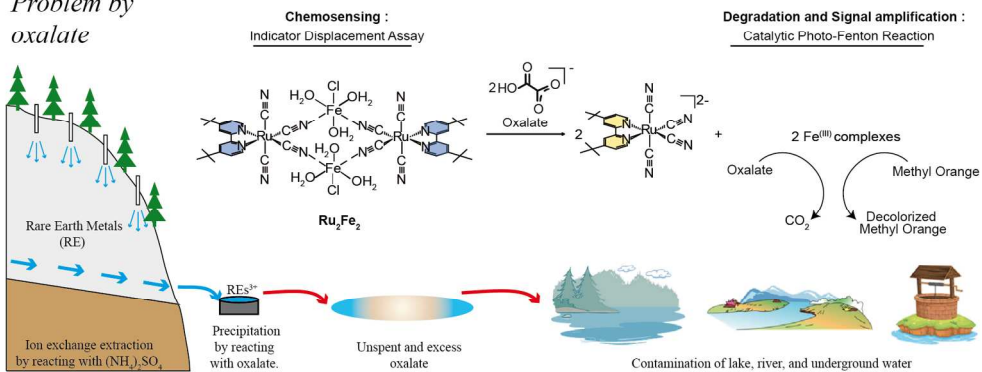
- (1) L. Ritter, K. Solomon, P. Sibley, K. Hall, P. Keen, G. Mattu, B. Linton, *J. Toxicol. Environ. Health* 2002, **65**, 1.
- (2) J. Fawell, M. J. Nieuwenhuijsen, *Br. Med. Bull.* 2003, **68**, 199.
- (3) D. D. Mara, *Public Health* 2003, **117**, 452.
- (4) B. Harris, *Trends Biotechnol.*, 1999, **17**, 290-296.
- (5) A. Vaseashta, M. Vaclavikova, S. Vaseashta, G. Gallios, P. Roy, O. Pummakarnchana, *Sci. Technol. Adv. Mater.*, 2007, **8**, 47.
- (6) S. Baruah, J. Dutta, *Environ. Chem. Lett.*, 2009, **7**, 191.
- (7) Y. Y. Liu, G. X. Su, B. Zhang, G. B. Jiang, B. Yan, *Analyst*, 2011, **136**, 872.
- (8) M. E. Moragues, R. Martinez-Manez, F. Sancenon, *Chem. Soc. Rev.*, 2011, **40**, 2593-2643.
- (9) B. T. Nguyen, E. V. Anslyn *Coord. Chem. Rev.*, 2006, **250**, 3118-3127.
- (10) J. L. Lavigne, E. V. Anslyn, *Angew. Chem. Int. Ed.*, 1999, **38**, 3666.
- (11) S. L. Wiskur, H. Ait-Haddou, J. J. Lavigne, E. V. Anslyn, *Acc. Chem. Res.* 2001, **34**, 963.
- (12) B. T. Nguyen, E. V. Anslyn, *Coord. Chem. Rev.* 2006, **250**, 3118.
- (13) L. Fabbri, A. Leone, A. Taglietti, *Angew. Chem. Int. Ed.*, 2001, **40**, 3066.
- (14) M. A. Hortala, L. Fabbri, N. Marcotte, F. Stomeo, A. Taglietti, *J. Am. Chem. Soc.*, 2003, **125**, 20.
- (15) V. Amendola, G. Bergamaschi, A. Buttafava, L. Fabbri, E. Monzani, *J. Am. Chem. Soc.*, 2010, **132**, 147.
- (16) D. Jimenez, R. Martinez-Manez, F. Sancenon, J. V. Ros-Lis, A. Benito, J. Soto, *J. Am. Chem. Soc.*, 2003, **125**, 9000.
- (17) R. Martinez-Manez, F. Sancenon, *Chem. Rev.* 2003, **103**, 4419.
- (18) M. E. Moragues, R. Martinez-Manez, F. Sancenon, *Chem. Soc. Rev.* 2011, **40**, 2593.
- (19) C. F. Chow, B. K. W. Chiu, M. H. W. Lam, W. Y. Wong, *J. Am. Chem. Soc.*, 2003, **125**, 7802.
- (20) C. F. Chow, M. H. W. Lam, W. Y. Wong, *Anal. Chem.*, 2011, **83**, 289.
- (21) C. F. Chow, M. H. W. Lam, W. Y. Wong, *Anal. Chem.*, 2013, **85**, 8246.
- (22) M. R. Hoffmann, S. T. Martin, W. Y. Choi, D. W. Bahnemann, *Chem. Rev.* 1995, **95**, 69.
- (23) S. Q. Liu, S. Cheng, L. R. Feng, X. M. Wang, Z. G. Chen, *J. Hazard. Mater.* 2010, **182**, 665.
- (24) Liu, S. Q.; Cheng, S.; Luo, L.; Cheng, H. Y.; Wang, S. J.; Lou, S. A. *Environ. Chem. Lett.* 2011, **182**, 31.
- (25) L. Zhu, E. V. Anslyn, *Angew. Chem. Int. Ed.*, 2006, **45**, 1190.
- (26) Q. Wu, E. V. Anslyn, *J. Am. Chem. Soc.*, 2004, **126**, 14682.
- (27) P. Scrimin, L. J. Prins, *Chem Soc. Rev.*, 2011, **40**, 4488-4505.
- (28) R. Bonomi, A. Cazzolaro, A. Sansone, P. Scrimin, L. J. Prins, *Angew. Chem. Int. Ed.*, 2011, **50**, 2307.
- (29) M. S. Baker, S. T. Phillips, *J. Am. Chem. Soc.*, 2011, **133**, 5170.
- (30) M. A. Swiderska, J.-L. Reymond, *Nature Chem.* 2009, **1**, 527.
- (31) M. S. Masar III, N. C. Gianneschi, C. G. Oliveri, C. L. Stern, S. T. Nguyen, C. A. Mirkin, *J. Am. Chem. Soc.*, 2007, **129**, 10149.
- (32) N. Graf, M. Goritz, R. Kramer, *Angew. Chem. Int. Ed.*, 2006, **45**, 4013.
- (33) J. P. Gosling, *Clin. Chem.* 1990, **36**, 1408.
- (34) W. Riemenschneider, M. Tanifuji, 2000. Oxalic Acid. Ullmann's Encyclopedia of Industrial Chemistry.
- (35) A. Sjode, S. Winstrand, N. O. Nilvebrant, L. J. Jonsson, *Enzyme Microb. Technol.* 2008, **43**, 78.
- (36) *Research Report of Chinese Oxalic Acid Industry* (China Research and Intelligence Company, 2009).
- (37) R. Von Burg, *J. App. Toxicol.*, 1994, **14**, 233.
- (38) G. P. Kasidas, G. A. Rose, *Clin. Chim. Acta.* 1986, **154**, 49.
- (39) L. C. Cao, J. Jonassen, T. W. Honeyman, C. Scheid, *Am. J. Nephrol.* 2001, **21**, 69.
- (40) V. Thamilselvan, M. Menon, S. Thamilselvan, *Am. J. Physiol.: Renal Physiol.* 2009, **297**, F1399-F1410.

- 
- 1 (41) Synthetic procedures and spectroscopic/spectrofluorimetric analyses are  
2 described in detail in the Supporting information.  
3 (42) M. B. Robin, P. Day, *Adv. Inorg. Chem. Radiochem.* 1967, **10**, 247.  
4 (43) T. Sheng, H. Vahrenkamp, *Eur. J. Inorg. Chem.* 2004, 1198.  
5 (44) C. A. Bignozzi, C. Chiorboli, M. T. Indelli, M. A. Rampi-Scandola, G.  
6 Varani, F. Scandola, *J. Am. Chem. Soc.*, 1986, **108**, 7872.  
7 (45) S. Campagna, S. Serroni, *Chem. Rev.* 1996, **96**, 759.  
8 (46) E. Rodriguez, F. J. Mimbreno, F. J. Masa, Beltran, *Water Res.* 2007, **41**,  
9 1325. M.  
10 (47) F. Wu, N. Deng, *Chemosphere*, 2000, **41**, 1137.  
11 (48) Y. Zuo, J. Holgne, *Atmos. Environ.*, 1994, **28**, 1231.  
12 (49) P. A. Fiorito, S. I. C. de Torresi, *Talanta*. 2004, **62**, 649.  
13 (50) E. F. Perez, G. D. Neto, L. T. Kubota, *Sens. Actuators, B.* 2001, **72**, 80.  
14  
15  
16  
17  
18  
19  
20  
21  
22  
23  
24  
25  
26  
27  
28  
29  
30  
31  
32  
33  
34  
35  
36  
37  
38  
39  
40  
41  
42  
43  
44  
45  
46  
47  
48  
49  
50  
51  
52  
53  
54  
55  
56  
57  
58  
59  
60

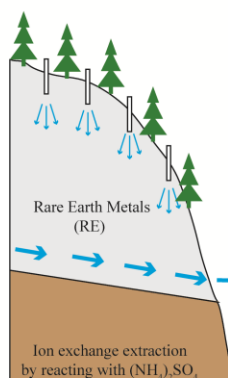
1  
2  
3  
4  
5  
6  
7  
8  
9  
10  
11  
12  
13  
14  
15  
16  
17  
18  
19  
20  
21  
22  
23  
24  
25  
26  
27  
28  
29  
30  
31  
32  
33  
34  
35  
36  
37  
38  
39  
40  
41  
42  
43  
44  
45  
46  
47  
48  
49  
50  
51  
52  
53  
54  
55  
56  
57  
58  
59  
60

*Environmental Problem by oxalate*

*Solving the Problem by:*

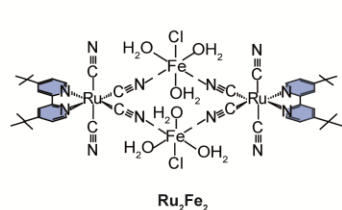


Environmental  
Problem by  
oxalate



Solving the Problem by:

Chemosensing :  
Indicator Displacement Assay



Degradation and Signal amplification :  
Catalytic Photo-Fenton Reaction

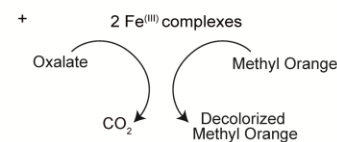


**Table of contents**

Multifunctional device that can monitor the level of pollutants, magnify weak signal, and subsequently degrade pollutants is highly desirable. A new Ru(II)–Fe(III) complex— $[\text{Ru}^{\text{II}}(\text{tBubpy})(\text{CN})_4]_2-[\text{Fe}^{\text{III}}(\text{H}_2\text{O})_3\text{Cl}]_2 \cdot 4\text{H}_2\text{O}$  (1,  $\text{tBubpy} = 4,4'$ -Di-*tert*-butyl-2,2'-bipyridine)—was synthesized and characterized.